

Electronic excitation induced modifications of nanostructured Ni-Ti shape memory alloy thin films

V. Kumar¹, R. Singhal^{1*}, R. Vishnoi², M. Gupta³, P. Sharma¹, M. K. Banerjee⁴, K. Asokan⁵, H. Sharma¹, A. Gupta⁶, D. Kanjilal⁵

¹Department of Physics, Malaviya National Institute of Technology Jaipur, JLN Marg, Malviya Nagar, Jaipur 302017, India

²Department of Physics, Vardhman College, Bijnor, U.P. 246701, India

³UGC-DAE Consortium for Scientific Research, University Campus, Khandwa Road, Indore 452001, India

⁴Department of Metallurgical and Materials Engineering, Malaviya National Institute of Technology Jaipur, JLN Marg, Malviya Nagar, Jaipur 302017, India

⁵Inter University Accelerator Centre, Aruna Asaf Ali Marg, New Delhi 110067, India

⁶Amity Center for Spintronic Materials, Amity University, Sector 125, Noida 201303, India

*Corresponding author, E-mail: rsinghal.phy@mnit.ac.in

Received: 11 October 2015, Revised: 25 July 2016 and Accepted: 06 September 2016

DOI: 10.5185/amlett.2017.6211

www.vbripress.com/aml

Abstract

In the present work, the effects of 120 MeV Au ion irradiation at different fluences ranging from 1×10^{12} to 3×10^{13} ions/cm² on structural and electrical properties of thin films of Nickel titanium (Ni-Ti) shape memory alloys (SMAs) grown on Si substrate using DC magnetron co-sputtering is studied. The surface morphology, crystallization and phase transformation behaviour of these films were investigated using field emission scanning electron microscopy (FESEM), atomic force microscopy (AFM), X-ray diffraction (XRD) and Four-terminal resistivity measurement method. XRD pattern reveals that both the phases-martensite as well as austenite exist in the pristine film. Resistivity measurements revealed a two way transformation from cubic to rhombohedral and from rhombohedral to monoclinic phase in pristine film and decrease in its transformation temperature with increased fluence. At higher fluences 5×10^{12} and 1×10^{13} ions/cm², films showed non-metallic behaviour which could be due to the disorder occurring in these films due to ion impact and precipitate formation. The elemental composition of pristine film is determined by Rutherford backscattering spectroscopy. Copyright © 2017 VBRI Press.

Keywords: SMA, NiTi, SHI irradiation.

Introduction

Nowadays, the demand for micromachines has increased significantly in various fields such as biotechnology, aerospace, micro-electro-mechanical systems (MEMS), industries and various biomedical applications [1-3]. Thin films of Ni-Ti alloy can be used to produce such microactuators because of their unique properties such as large stress sustainability without deforming permanently [4], low voltage controllability, biocompatibility, shape memory behaviour etc. Also, the work output per unit volume of these films is quite large as compared to other micro-actuation mechanisms [5]. Recently, NiTiCu based ultralow-fatigue SMA films containing Ti₂Cu precipitates for 10 million transformation cycles were reported for artificial heart valve or elastocaloric cooling [6]. These unique properties in Ni-Ti films are due to their distinct crystalline structure (B2 at high temperature exhibiting austenite phase and monoclinic at low temperature

exhibiting martensite phase) and phase transformation behaviour. The phase transformation is accompanied by significant changes in the structural and electrical properties of films, thus controlling the design and fabrication of micro-actuators and out of several methods one of the effective ways to produce phase transformation in shape memory alloys is high energy ion irradiation.

The effect of different type of perturbations such as ion beam irradiation, electron irradiation and proton irradiation on shape memory alloys has been investigated by many groups. Moine *et al.* studied 250 and 390 keV Ni ions implantation induced amorphization on bulk martensitic Ti-Ni alloy [7]. It was reported that at a temperature of 300 K, the fluence required to transform the martensitic transformation to amorphous state was 0.1 dpa whereas at a temperature of 77 K, the required dose was found to be on high side ~ 0.18 dpa and the reasoning was given in terms of the stabilization of martensite phase at lower temperature. Another report

was given by Brimhall *et al.*, who irradiated the Ni-Ti alloy by 2.5 MeV Ni ion beam and 6 MeV Ti ion beam at a dose of ~ 0.2 dpa and observed a complete amorphization of Ni-Ti austenitic phase after ion irradiation [8]. They concluded that amorphization of the phase was possible without complete chemical disordering. Zu *et al.* observed the amorphization of Ti-Ni-Cu alloy samples which were irradiated by 400 keV Xe ions at a dose of 0.4 dpa [9]. Vishnoi *et al.* observed phase transformation at low fluence (6×10^{12} ions/cm²) and amorphization at high fluence (3×10^{13} ions/cm²) in Ni-Mn-Sn ferromagnetic SMA thin films using 200 MeV Au ions [10] while Singhal *et al.* observed phase transformation at slightly higher fluence (1×10^{13} ions/cm²) in Ni-Mn-Sn film of different composition using 120 MeV Ag ions [11]. Pelletier *et al.* studied the phase transformation in Ni-Ti wire by using 1.5 MeV Ar ions to increase the life time of endodontic instrument. They observed the completely amorphization of martensite phase at a fluence of 5×10^{17} ions/cm², while the austenite phase was partially amorphized [12]. Lagrange *et al.* also studied the suppression of martensite phase in Ni-Ti thin films irradiated by 5 MeV Ni ions to develop the shape memory thin films actuator. They observed that martensite phase was first transformed into austenite phase and then become amorphized [13]. Ikenaga *et al.* studied 3 MeV Cu ion implanted bulk Ti-Ni films and they observed amorphous region at a fluence of 10^{14} ions/cm² at 300 K substrate temperature, but in case of 100 K it did not appear even at 10^{15} ions/cm² [14]. They observed that the sample implanted at 100 K, ion implanted region showed crystallinity however sample implanted at 300 K modified to amorphous.

It is well understood from these studies that the properties of SMA can be significantly modified using ion irradiation techniques. Among all types of ion irradiation, SHI irradiation is of special significance since SHI is a very useful tool for modifying the properties of films, foils and surface of bulk solids. SHI transfers its energy to the material mainly by inelastic collision which causes electronic excitation of the atoms in the material and produces long narrow disordered region along its path called track whose length and diameter depend on the types and energy of ion beam used to irradiate the material. The mechanism of transfer of electronic excitation to the displacement of lattice atoms could be understood by commonly known models such as Coulomb explosion model [15] and thermal spike model [16]. Though, it is difficult to produce tracks in metals due to the large number of mobile conduction electrons present in them which shield the space charge produced by the ionization of metal atoms by incoming swift heavy ions and by spreading the energy deposited by these ions very rapidly, however, formation of tracks by heavy ions was reported in metals such as Ni₃B [17], NiZr₂ [18], Ni-Ti [19] shape memory alloy etc.

Thus, with reference to the above mentioned studies and to the best of our knowledge, there are few reports of SHI irradiation on bulk Ni-Ti but there are no such reports in case of Ni-Ti metallic thin films which are very much

needed to understand the effects of SHI interaction with Ni-Ti films since they are more promising candidates for various applications as compared to bulk due to their various distinguished characteristics and to explore how the transformation temperatures can be controlled by ion irradiation making them useful for different applications.

Therefore, in this study, we report the preliminary work done by using SHI irradiation on Ni-Ti films. The present work is focussed on ion-beam induced modifications of 120 MeV Au ion irradiated Ni-Ti sputter deposited thin films which are investigated using X-ray diffraction, Rutherford Backscattering spectroscopy, atomic force microscopy, Field emission scanning electron microscopy and Electrical resistivity measurements.

The main objective of the present study is to investigate the effects of SHI on both phases, austenite as well martensite phase simultaneously at room temperature for the future application of these material in harsh environment such space or nuclear reactor. In present experiment, we also investigated the critical value of fluence for shape memory behaviours. Below this critical fluence Ni-Ti films show the SMA behaviour. Irradiation at low fluence below the critical value creates the defect in the materials in a control manner which increase the vacancies diffusion and this diffusion of vacancies lead to higher mobility.

The schematic of the work presented in manuscript is shown in Fig. 1. The modifications in the structural and electrical properties against SHI at different ions fluences of 120 MeV energy were characterized by FESEM, AFM, RBS, XRD and four-terminal resistivity measurement. The measurement showed the disorder produced in microstructure in Ni-Ti films strongly dependent upon the ion fluences and at a higher fluence of 3×10^{13} ions/cm², both phase's austenite as well as martensite was completely disappeared due to huge amount of electronic energy deposited by SHI in Ni-Ti matrix.

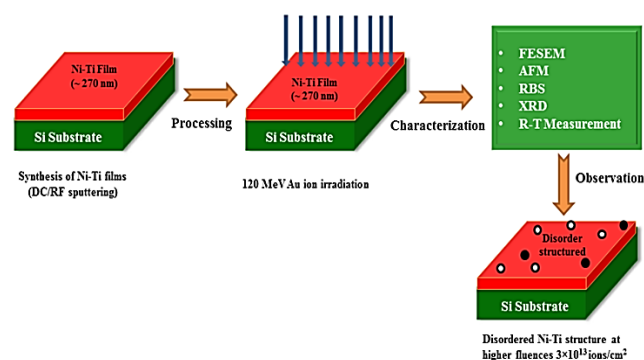


Fig. 1. Schematic diagram of Ni-Ti thin films deposited at 550 °C and irradiated at different fluences.

Experimental

Ni-Ti films were deposited by direct current magnetron sputtering technique on Si substrates by using an AJA Int. Inc. make ATC Orion-8 series sputtering system. Two separate targets of Ni and Ti were used for thin film deposition. The arrangement of rotation of substrate in

horizontal plane was also possible during film deposition for better uniformity. The substrates were first cleaned in an ultrasonic bath using a mixture of distilled water and trichloroethylene in 4:1 ratio and then they were washed with acetone. High purity nickel (99.9%, 50 mm diameter and 2 mm thickness) and titanium (99.9%, 50 mm diameter and 3 mm thickness) targets were used for film deposition. The Ar pressure was regulated to be 0.13 Pa. The target to substrate distance was fixed approximately 16 cm. Before deposition, a base pressure of 2×10^{-7} Torr was achieved and sputter cleaning of both the Si substrate and target (Ni at 50 W and Ti at 100 W for 10 minutes) was done. After cleaning, the deposition was performed for 1 hour 40 minutes using direct current powers of 50 W for Ni and 100 W for Ti. During deposition, the pressure was kept constant at 3×10^{-3} Torr using a dynamic throttling valve and substrate temperature was kept constant at 550°C. Substrate holder was rotated at 60 rpm in a horizontal plane to deposit films of uniform composition. The thickness of all the deposited films was approximately 270 nm. Post-annealing was not performed after film deposition. These Ni-Ti films on Si substrate were irradiated with 120 MeV Au ion beam at IUAC New Delhi, India using 15 UD pelletron accelerator facility. Ion fluence was varied from 1×10^{12} to 3×10^{13} ions/cm². The electronic energy loss S_e and nuclear energy loss S_n calculated for Ni-Ti SMA using 120 MeV Au ions was $\sim 3.1 \times 10^3$ and 5.3×10^1 eV/Å, respectively, and the range of Au ions in Ni-Ti was ~ 7.6 μm as calculated by SRIM programme [20], which was found to be much higher than the film thickness, so most of the Au ions after passing through the film get buried into the Si substrate.

The surface morphology and microstructure of the films were studied using FESEM (Nova Nano FE-SEM 450 FEI) and AFM using a Bruker make Nanoscope v system with a Si₃N₄ cantilever in noncontact mode. The thickness and elemental composition of the films were measured using Rutherford backscattering spectrometer. The orientation, crystallinity and room temperature phase of the pristine and irradiated films were studied using X-ray diffractometer (Bruker D8 Advance) equipped with Cu Kα x-ray source in θ -2 θ geometry having a scan speed of 0.6 °/min. The electrical resistivity of Ni-Ti films at different temperatures was measured using four probe method over a temperature range from 100 to 400 K. The temperature of the film was measured by using Lake Shore thermocouple and temperature ramp was set at 2 K/minute during heating and cooling cycles. The contacts on the films were made by using silver paint.

Results and discussion

Structural properties

Field emission scanning electron microscopy

The surface properties of pristine and 120 MeV ion irradiated Ni-Ti films were determined by FE-SEM. Fig. 2(a) to 2(e) show the FE-SEM micrographs of pristine and irradiated films at different fluences ranging from 1×10^{12} to 3×10^{13} ions/cm². It is clear from these

images that different shaped grains such as pyramidal and spherical, are formed and the grain size first increases with increase in the ion fluence, remain constant up to a certain fluence and then decreases first gradually and then considerably with further increase in the fluence. Fig. 2(a) shows that in the pristine film pyramidal and spherical shaped grains are observed depicting the presence of both austenite and martensite phases in the films. But, the pyramidal grains are quite large in number as compared to spherical grains due to the dominance of austenite phase in the film. Fig. 2(b) shows diffused pyramidal and spherical grains present in the film irradiated at a fluence of 1×10^{12} ions/cm². The grain size increases but the number of pyramidal grains decreases while that of spherical grains increases due to the decrease of austenite phase and slight increment of martensite phase in the film in accordance with the XRD data which is later shows decrease in the intensity of (110) peak depicting austenite phase while broadening and slight increase in the intensity of (002) peak depicting martensite phase. With increase in fluence to 5×10^{12} ions/cm² (Fig. 2(c)), FESEM micrograph show grains of similar morphology and constant size as found in film irradiated at fluence 1×10^{12} ions/cm². At further increased fluence of 1×10^{13} ions/cm², smaller grains with diffused grain boundaries are observed (Fig. 2(d)). As the fluence is increased to 3×10^{13} ions/cm² (Fig. 2(e)), the grain size decreases considerably to the extent that surface morphology of the film completely disappears and a smooth film appears which may be due to the amorphization of the film at a fluence of 3×10^{13} ions/cm².

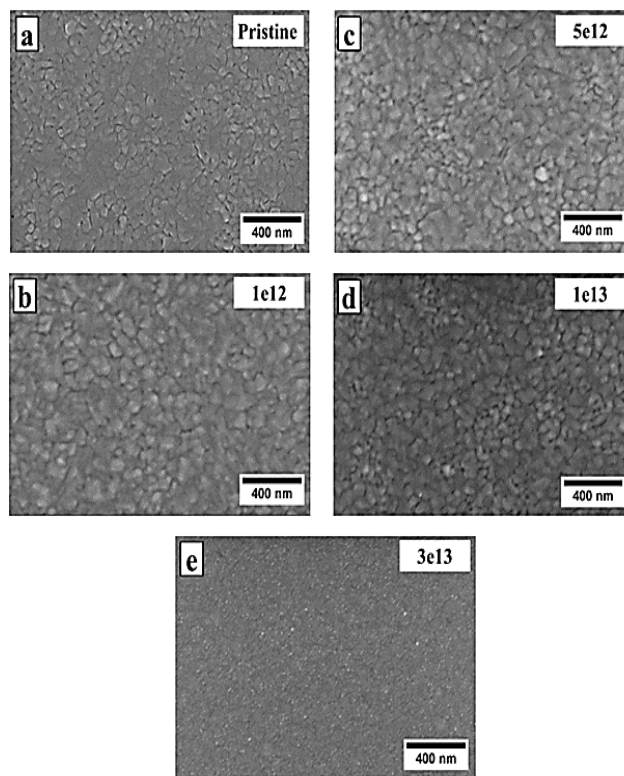


Fig. 2. FESEM images of pristine and 120 MeV Au ion irradiated Ni-Ti thin films at different fluences.

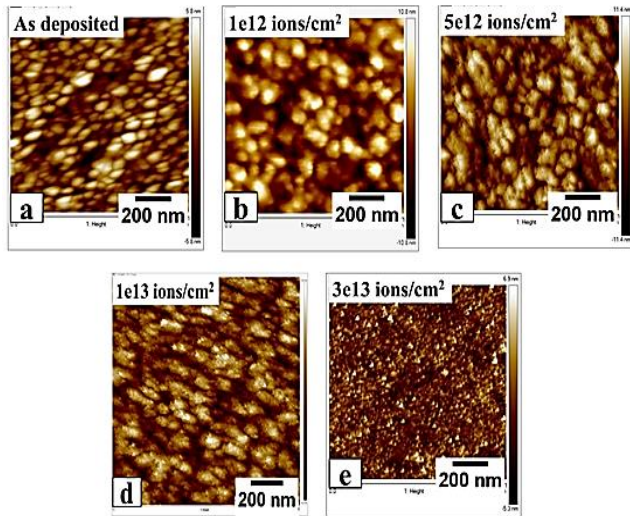


Fig. 3. AFM images of pristine and 120 MeV Au ion irradiated Ni-Ti thin films at different fluences.

Atomic force microscopy

Apart from FESEM, the surface morphology (grain size and surface roughness) of all the films was also analyzed using AFM. **Fig. 3(a)** to **(e)** shows the two dimensional AFM images of as- deposited and 120 MeV Au ion irradiated Ni-Ti SMA films at a scale of $1\mu\text{m}\times 1\mu\text{m}$. The root-mean-square roughness (R_{rms}) of the surfaces of the films was obtained from AFM scans over film areas of $2\mu\text{m}\times 2\mu\text{m}$ by scanning three times, each time at a different location for every film. R_{rms} of the films was calculated using the following formula,

$$R_{\text{rms}} = \sqrt{\frac{\sum z_i^2}{N}}$$

where, R_{rms} is the root mean square roughness taken from the mean image data plane and Z_i is the current Z value, Z is the Peak-to-valley difference in height values within the analyzed region, N is the number of points within the box cursor in nm. The average values of surface roughness of as deposited and irradiated films at different fluences 1×10^{12} , 5×10^{12} , 1×10^{13} and 3×10^{13} ions/cm² was found to be ~ 2.9 nm, ~ 3.98 nm, ~ 3.85 nm, ~ 3.76 nm and 1.88 nm respectively. It was observed that root mean square surface roughness first increases with increase in fluence to 1×10^{12} ions/cm² due to the increased intensity of martensite phase in the film and then it again decreases but to a smaller extent for films irradiated at 5×10^{12} and 1×10^{13} ions/cm² respectively, whereas it decreases considerably for film irradiated at 3×10^{13} ions/cm² due to the complete amorphization of the film resulting in the disappearance of both the austenite and martensite phases, in accordance with the FESEM result as reported in **Fig. 2**. The sizes of the grains calculated by AFM also show similar behaviour as calculated by FESEM images.

Rutherford backscattering spectroscopy

The major problem in using Ni-Ti films for various applications is the difficulty in controlling their chemical

composition. The transformation temperatures of Ni-Ti also depend considerably on the composition of films. A slight change in the composition results in a remarkable change in the transformation temperatures and thus the various properties of the films.

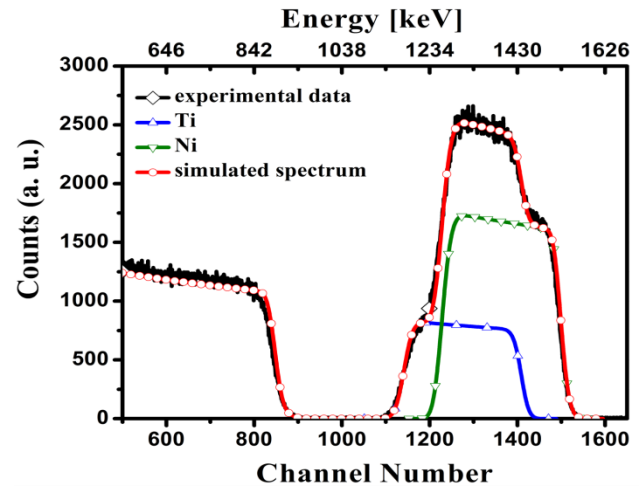


Fig. 4. RBS spectra (2 MeV He⁺) performed on as deposited film shows Ni and Ti edges for the channel number in the range of 1100-1500 range.

So formation of desired composition in the films and also accurate determination of composition in the films after formation is very essential. Rutherford backscattering spectroscopy (RBS) is an efficient method to determine the composition of the films as well as film thickness, atomic species present in the films and their concentration. **Fig. 4** shows Rutherford backscattering spectrum of as deposited Ni-Ti film on Si substrate. In order to measure the film thickness and to determine the atomic concentration of metals in the film, the RBS spectrum was simulated by SIMNRA [21], and a fit is shown in **Fig. 4** by continuous line. The Ni atomic fraction was calculated 56.7 at. % and Ti was found to be 43.3 at. %. The film thickness simulated by SIMNRA was found to be ~ 270 nm.

X-ray diffraction

Fig. 5 shows the room temperature X-ray diffraction (XRD) pattern of Ni-Ti pristine film and also of the films irradiated by 120 MeV Au ions at different fluences ranging from 1×10^{12} to 3×10^{13} ions/cm². In addition to substrate peak, XRD pattern reveals that both the phases, austenite (B2) as well as martensite (B19') exist in the pristine sample. No traces of other phases like Ti₂Ni and Ti₃Ni₄ were observed in XRD pattern of these films. The planes corresponding to austenite and martensitic structure are marked by their Miller indices. The most intense peak at $2\theta=42.5^\circ$ which is due to the (110) fundamental reflection corresponds to cubic austenite structure, and the peak at $2\theta=43.9^\circ$ which is due to (002) fundamental reflection corresponds to monoclinic martensite structure. The peaks ($\bar{1}36$), ($1\bar{3}6$) and (0 $\bar{4}4$) corresponds to naturally oxidized Si substrate. The film irradiated at a fluence of 1×10^{12} ions/cm² shows decrease

in the intensity of (110) peak (corresponding to B2 phase) and the (002) peak, corresponding to B19', becomes broad. It indicates the damage of austenite structure in the film upon ion irradiation. With increase in the fluence to 5×10^{12} ions/cm², the peak intensity of both the phases decreases. With further increase in fluence to 1×10^{13} ions/cm², the intensity of these peaks decreases considerably. The decrease in intensity of both the phases at this fluence shows the partial amorphization of the austenite and martensite phase and suppression of phase transformation by the electronic energy deposition in Ni-Ti regime. At a much higher fluence of 3×10^{13} ions/cm², all the peaks are vanished and the film gets completely amorphized due to excessive ion impact. Amorphization by electronic excitation and ionization is also possible, where the energy of the incoming ion is transferred to the atoms of lattice via electron-electron and electron-phonon coupling. Such electron excitations can also cause local heating followed by a rapid quenching (thermal spikes) producing lattice distortions which are so drastic that they relax into an amorphous state [22].

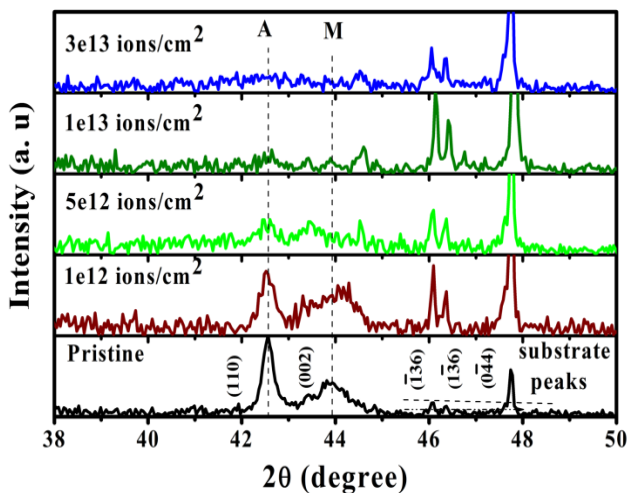


Fig. 5. X-ray diffraction spectra of pristine and 120 MeV Au ion irradiated Ni-Ti thin films at different fluences.

The XRD pattern shows the crystalline to amorphous phase transformation of Ni-Ti thin films by SHI irradiation at a fluence of 3×10^{13} ions/cm². The suppression of both the phases under the SHI irradiation has been observed by introduction of lattice defects and high strain generation by the bombardment of Au ions on Ni-Ti films. The amorphization of materials depends on the irradiation conditions such as ion fluence, irradiation temperature and nature of the ions as reported by several authors [23, 24]. In the case of electron and proton irradiation, it has been well established in the literature that irradiation cause stress field and lattice disorder in the materials [25]. The lattice disorder by electronic excitation produces the point defect (vacancy and interstitial pairs) which is evenly distributed in the material and suppress the transformation temperature and cause amorphization. Irradiation at critical fluences, produce isolated amorphous zone in a crystalline material

and density of these amorphous zones is continuously increased with increase the fluences and at a higher fluence these amorphous zone starts to overlap and at a critical fluence, material become amorphous.

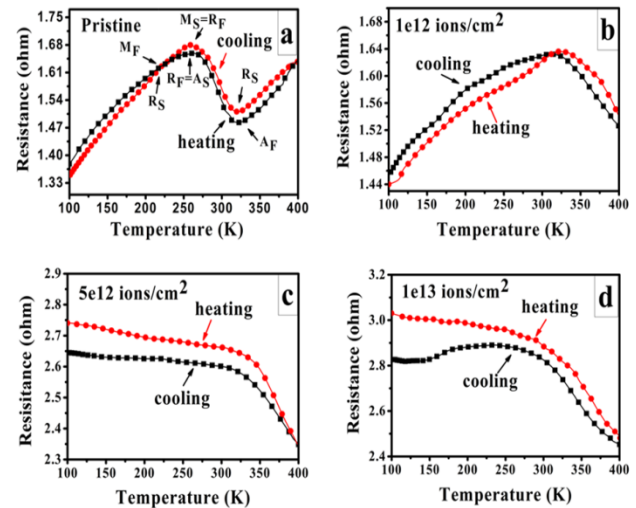


Fig. 6. Electrical resistance versus temperature (R-T) curves of pristine and 120 MeV Au ion irradiated Ni-Ti films, during heating and cooling cycle.

Electrical properties

The variation of electrical resistance with temperature is an effective method for determining the formation of various phases in shape memory alloys thin films and studying their phase transformation behaviour since the high temperature ordered austenite phase, intermediate R phase and low temperature disordered martensite phases are accompanied with changes in the electrical resistance due to their different crystal structures.

Fig. 6(a) to (d) show the electrical resistance versus temperature curves of pristine and 120 MeV Au ion irradiated Ni-Ti films, measured by four-terminal resistivity method during cooling and heating cycles in the temperature range 100-400 K. At the time of experiment, the condition of stationary equilibrium was maintained by cycling the temperature stepwise with a sufficient time interval at every data point. In figures 6(a) to (d) R_s , R_f , M_s , M_f and A_s , A_f denote the start and finish temperatures of formation of the intermediate R phase and martensitic (B19') phase on cooling, and austenitic (B2) transformation on heating, respectively. Fig. 6(a) shows the electrical resistance versus temperature (R-T) curve of pristine Ni-Ti film. The pristine film shows a very clear two-step phase transformation $B2 \leftrightarrow R \leftrightarrow B19'$ during heating and cooling cycles. During heating cycle, electrical resistance of B2 phase was observed to increase with increase in the temperature because of the formation of R phase, but during cooling below 400 K, first the resistance value of B19' phase decreases linearly because of decrease in the intensity of electron-phonon interaction but at temperature below R_s (310 K), the electrical resistance again starts increasing with temperature because the austenite B19' phase gets distorted and starts transforming to R phase with higher electrical resistance,

because in small sized grains the restriction imposed by the grain boundaries for the formation of R phase is small as compared to that offered for phase transformation from austenite to martensite phase [26]. On cooling the film further below R_f (260 K), the electrical resistance goes on decreasing with temperature because R phase to martensite transformation begins to occur which gets completed below M_f . Thus, during both heating and cooling cycles, formation of R phase was observed which possess higher electrical resistance in comparison to B2 and B19' phases. Fig. 6(b) shows the R-T curve of thin film irradiated at a fluence 1×10^{12} ions/cm², in which slightly different trend of electrical resistance was observed upon ion irradiation with 120 MeV Au ions. It was observed that irradiated film showed deteriorated hysteresis as compared to pristine film. Also, the R-T curves during heating and cooling cycles do not show the clear phase transformation behaviour. It could be due to the disorder occurring in the film due to ion impact as also confirmed by the decrease in intensity of ordered austenite phase from XRD data. R-T curves of films irradiated at fluences 5×10^{12} and 1×10^{13} ions/cm² as shown in figures 6(c) and (d) show the non-metallic behaviour of both the films without any indication of phase transformation during subsequent heating and cooling cycles. At higher fluence (1×10^{13} ions/cm²) the energy deposited by incoming ions in the film due to the electronic stopping is quite large and leads to degradation of shape memory behaviour and complete amorphization of the films. In the present case, the incomplete phase transformation could be attributed to the following reasons; (a) large resistance force as compared to driving force could be generated due to the constraints imposed by inter-diffusion of film and substrate due to ion irradiation (b) large number of grain boundaries due to small grain size restrict the growth of martensitic phase during cooling (c) presence of intrinsic defects created by 120 MeV Au ions in Ni-Ti thin films at higher fluences.

Conclusion

In this study, a systematic and preliminary investigation on the effect of 120 MeV Au ions irradiation at different fluences ranging from 1×10^{12} to 3×10^{13} ions/cm² on Ni-Ti SMA thin films deposited by DC-magnetron co-sputtering system on Si substrate at 550 °C was carried out. FESEM and AFM micrographs revealed the successive changes in the surface morphology of the films with increase in fluence content. As the fluence increases, spherical shaped grains increases as compared to pyramidal ones due to change in phase and at considerable higher fluence of 3×10^{13} ion/cm², spherical grains also disappear due to the amorphization of the films at such high fluence. XRD measurements revealed the presence of both the phases, austenitic as well as martensitic phase in pristine sample. As the fluence of 120 MeV Au ion increases, crystallinity of the Ni-Ti SMAs decreases and at a fluence of 3×10^{13} ions/cm² complete amorphization occurred. The R-T measurements revealed that clear phase transformation from martensite to austenite phase and vice versa via R-

phase was observed in pristine film during subsequent heating and cooling cycles. The R-T measurements also revealed the degradation of shape memory effect and occurrence of non-metallic behaviour of Ni-Ti films irradiated at higher fluences.

This study paved the way for exploring how the crystallinity and phase transformation temperatures of Ni-Ti nanocrystalline thin films can be controlled using ion irradiation in order to utilize them for applications.

Acknowledgements

One of the authors (V. Kumar) is thankful to the Technical Education Quality Improvement Programme (TEQIP), MNIT Jaipur for financial assistantship. The crew of Pelletron Accelerator group of IUAC New Delhi is highly acknowledged for providing stable beam of 120 MeV Au ions. Authors would like to acknowledge the help and support provided by Mr. Sunil Ojha for RBS measurements at IUAC New Delhi. Author is also thankful to UGC-DAE CSR Indore for synthesis of Ni-Ti thin films, and Materials Research Centre, MNIT Jaipur for providing characterization techniques such as AFM and FESEM. One of the authors (R. Singhal) highly acknowledges the financial support provided by DST New Delhi in terms of DST FAST Young Scientist project (SR/FTP/PS-081/2011). One of the authors (R. Vishnoi) highly acknowledges the financial support provided by DST New Delhi in terms of DST FAST Young Scientist project (SR/FTP/PS-029/2012).

References

1. Humbeeck, J. V. ; *Adv. Eng. Mater.* **2001**, 3, 837.
DOI: [10.1002/1527-2648\(200111\)3:11<837::AID-ADEM837>3.0.CO;2-0](https://doi.org/10.1002/1527-2648(200111)3:11<837::AID-ADEM837>3.0.CO;2-0)
2. Humbeeck, J. V, Stalmans, R.; Wiley: **2002**, 951.
DOI: [10.1002/0471216275.esm073](https://doi.org/10.1002/0471216275.esm073)
3. Gill, J. J, Chang, D. T, Momoda, L. A, Carman, G. P.; *Sens. Actuat. A. Phys.*, **2001**, 93, 148.
DOI: [10.1016/S0924-4247\(01\)00646-X](https://doi.org/10.1016/S0924-4247(01)00646-X)
4. Bush, J. D., Johnson, A. D., Lee, C. H., Stevenson, D. A.; *J. Appl. Phys.*, **1990**, 68(12), 6224.
DOI: [10.1063/1.346914](https://doi.org/10.1063/1.346914)
5. Krulevitch, P., Lee, A. P., Ramsey, P. B., Trevino, J. C., Hamilton, J., Northp, M. A.; *J. Microelectro-mech. Syst.*, **1996**, 5, 270.
DOI: [10.1109/84.546407](https://doi.org/10.1109/84.546407)
6. Chluba, C., Ge, W., Miranda, R. L. De, Strobel, J., Kienle, L., Quandt, E., Wuttig, M.; *Science*, **2015**, 348, 1004.
DOI: [10.1126/science.1261164](https://doi.org/10.1126/science.1261164)
7. Moine, P.; Jaoen, C. *J. Alloys Compd.* **1993**, 194, 373.
DOI: [10.1016/0925-8388\(93\)90022-F](https://doi.org/10.1016/0925-8388(93)90022-F)
8. Brimhall, J., Kissinger, H., Pelton, A.; *Radiat. Eff. Defects Solids*, **1985**, 90, 241.
DOI: [10.1080/00337578508222535](https://doi.org/10.1080/00337578508222535)
9. Zu, X. T., Zhu, S., Xiang, X., You, L. P., Huo., Y., Wang, L. M.; *Mater. Sci. Eng., A*, **2003**, 36, 352.
DOI: [10.1016/S0921-5093\(03\)00635-X](https://doi.org/10.1016/S0921-5093(03)00635-X)
10. Vishnoi, R., Singhal, R., Asokan, K., Kanjilal, D., Kaur, D.; *Appl. Phys. A*, **2012**, 107, 925.
DOI: [10.1007/s00339-012-6826-5](https://doi.org/10.1007/s00339-012-6826-5)
11. Singhal, R., Vishnoi, R., Asokan, K., Kanjilal, D., Kaur, D.; *Vacuum*, **2013**, 89, 215.
DOI: [10.1016/j.vacuum.2012.05.017](https://doi.org/10.1016/j.vacuum.2012.05.017)
12. Pelletier, H., Muller, D., Millea, P., Grob, J. J.; *Surface and Coatings Technology*, **2002**, 301, 158.
DOI: [10.1016/S0257-8972\(02\)00187-1](https://doi.org/10.1016/S0257-8972(02)00187-1)
13. LaGrange, T., Gotthardt, R.; *Scripta Materialia*, **2004**, 50, 231.
DOI: [10.1016/j.scriptamat.2003.09.017](https://doi.org/10.1016/j.scriptamat.2003.09.017)
14. Ikenaga, N., Kishi, Y., Yajima, Z., Sakudo, N., Nakano, S., Ogiso, H.; *Nucl. Instrum. Methods Phys. Res., Sect. B*, **2009**, 267, 1509.
DOI: [10.1016/j.nimb.2009.01.077](https://doi.org/10.1016/j.nimb.2009.01.077)

15. Leuser, D., Dunlop, A.; *Radiat. Eff. Defects Solids*, **1993**, 126, 163.
DOI: [10.1080/10420159308219701](https://doi.org/10.1080/10420159308219701)
16. Szenes, G.; *Phys. Rev. B*, **1995**, 51, 8026.
DOI: <http://dx.doi.org/10.1103/PhysRevB.51.8026>
17. Audouard, A., Balanzat, E., Bouffard; Jousset, J. C., Chamberod, A., Dunlop, A., Lesueur, D., Fuchs, G., Spohr, R., Vetter; *J. Phys. Rev. Lett.*, **1990**, 65, 875.
DOI: <http://dx.doi.org/10.1103/PhysRevLett.65.875>
18. Barbu, A., Dunlop, A., Lesueur, D., Averback, R. S.; *Europhys. Lett.* **1991**, 15, 37.
DOI: <http://dx.doi.org/10.1209/0295-5075/15/1/007>
19. Dunlop, A., Lusueur, D., Barbu; *A. J. Nucl. Mater.*, **1993**, 205, 426.
DOI: [10.1016/0022-3115\(93\)90106-9](https://doi.org/10.1016/0022-3115(93)90106-9)
20. Zeigler, J. F., Biersack, J. P.; Springer US: New York, **1985**.
DOI: [10.1007/978-1-4615-8103-1_3](https://doi.org/10.1007/978-1-4615-8103-1_3)
21. Adeoya, O, Ali, M. H., Muller, J. C., Siffert, P., *Appl. Phys. Lett.*, **1987**, 50, 1736.
DOI: [10.1063/1.97732](https://doi.org/10.1063/1.97732)
22. Lagrange, T., Schaublin, R., Grummon, D. S., Abromeit, C., Gotthardt, R.; *Philos. Mag.*, **2005**, 85, 577.
DOI: [10.1080/02678370412331320107](https://doi.org/10.1080/02678370412331320107)
23. Moine, P., Rivieri, J. P., Chaumont, J., Pelton, A., Sinclair, R.; *Nucl. Instrum. Methods Phys. Res., Sect. B*, **1985**, 7-8, 20.
DOI: [10.1016/0168-583X\(85\)90523-3](https://doi.org/10.1016/0168-583X(85)90523-3)
24. Czeppe, T., Zayonts, N. L., Swiatek, Z., Michalec, M., Bonchik, O., Savitskij, G.; *Vacuum*, **2009**, 83, S214.
DOI: [10.1016/j.vacuum.2009.01.066](https://doi.org/10.1016/j.vacuum.2009.01.066)
25. Matsukawa, Y., Ohnuki, S.; *Journal of Nuclear Materials*, **1996**, 239, 261.
DOI: [10.1016/S0022-3115\(96\)00428-X](https://doi.org/10.1016/S0022-3115(96)00428-X)
26. Waitz, T., Kazykhanov, V., Karnthaler, H. P.; *Acta Mater.*, **2004**, 52, 137.
DOI: [10.1016/j.actamat.2003.08.036](https://doi.org/10.1016/j.actamat.2003.08.036)

A Monthly Journal

Publish your article in this journal

Advanced Materials Letters is an official international journal of International Association of Advanced Materials (IAAM, www.iaamonline.org) published monthly by VBRI Press AB from Sweden. The journal is intended to provide high-quality peer-review articles in the fascinating field of materials science and technology particularly in the area of structure, synthesis and processing, characterisation, advanced-state properties and applications of materials. All published articles are indexed in various databases and are available download for free. The manuscript management system is completely electronic and has fast and fair peer-review process. The journal includes review article, research article, notes, letter to editor and short communications.

Copyright © 2017 VBRI Press AB, Sweden www.vbripress.com/aml